Single Molecule Observations of Desorption-Mediated Diffusion at the Solid-Liquid Interface

Robert Walder, Nathaniel Nelson, and Daniel K. Schwartz*

Department of Chemical and Biological Engineering, University of Colorado, Boulder, Colorado 80309, USA

(Received 20 July 2011; published 7 October 2011)

By directly observing molecular trajectories on a chemically heterogeneous surface, we have identified two distinct modes of diffusion involving (1) displacements within isolated surface islands (crawling mode), and (2) displacements where a molecule desorbs from an island, diffuses through the adjacent liquid phase, and readsorbs on another island (flying mode). The diffusion coefficients corresponding to these two modes differ by an order of magnitude, and both modes are also observed on chemically homogeneous surfaces. Comparison with previous results suggested that desorption-mediated diffusion is the primary transport mechanism in self-assembled monolayer formation.

DOI: 10.1103/PhysRevLett.107.156102 PACS numbers: 68.35.Fx, 68.43.Jk, 68.47.Pe, 87.80.Nj

The mobility of molecules at the solid-liquid interface is of critical importance to several applications of surface science, including self-assembled monolayer growth [1,2], surface reactivity [3,4], and molecular recognition associated with both biomembranes and biosensors [5–7]. In these applications, a fundamental issue involves the way in which a molecule identifies a target on a surface. If molecular-surface transport is slow, then direct adsorption from solution onto the target is, by default, the dominant mechanism for molecular targeting. As surface mobility increases, both the magnitude and mechanism of diffusion becomes important for molecular targeting. For example, heterogeneous surfaces can have spatial barriers to purely surface-bound diffusion [8]. However, if adsorbate molecules can undergo desorption-mediated surface diffusion [9], then molecules can ''fly'' over these barriers.

The flying diffusion mechanism is particularly important for molecular targeting with low solution concentrations (and, consequentially, low adsorption rates), since the magnitude of diffusion is significantly larger than purely surface-bound diffusion. The larger diffusion coefficient allows the molecules to ''explore'' larger areas of the surface to find a target. With increasing solute concentrations, adsorption or desorption rates will become increasingly important; however, previous theoretical work suggests that surface diffusion still remains a critically important factor in determining the efficiency of targeting under relevant conditions [6,7]. Also, even at arbitrarily high solute concentrations, the flying mode will still increase the rate of any kinetic process in which surface diffusion is important, such as in the formation of self-assembled monolayers [1,2].

While some phenomena associated with the solid-liquid interface (e.g., adsorption and desorption) share many commonalities with those of other interfaces, the immobile nature of the solid phase creates a unique situation with respect to molecular mobility. In particular, the dominant qualitative mechanism of molecular diffusion at a gas-liquid [10–16] or liquid-liquid [10,17–22] interface is directly analogous to diffusion within a homogeneous fluid medium, involving Brownian motion amidst mobile solvent molecules. On a solid surface, however, an adsorbate molecule must ''detach'' to some degree in order to relocate. In general, two competing pictures have been used to describe this process. In the dominant paradigm, molecular mobility is considered an activated process consisting of a series of ''hops'' between localized binding sites that are separated by small energy barriers [8,23,24]. In this picture, the binding sites are spatially separated by atomic or molecular length scales. O'Shaughnessy and co-workers considered an alternative model, called desorption-mediated diffusion, where adsorbate molecules are imagined to detach completely from the interface, diffuse through the liquid phase, and readsorb at the interface [9]. They suggested that under some conditions, this mechanism of interfacial diffusion may be dominant, and theoretically described the statistical details of such a hypothetical mode, showing that it would lead to anomalous diffusion, including long flights. To date, it has proven difficult to directly test this prediction. In principle, of course, both types of diffusion may be operative simultaneously.

It is challenging to study surface diffusion under conditions where other surface processes are occurring simultaneously. Under special conditions, fluorescence recovery after photobleaching (FRAP) can be used to study the surface diffusion [25] of adsorbates in contact with aqueous solution. In general, however, it is impossible to unambiguously separate the fluorescence recovery associated with lateral diffusion from that due to adsorption and desorption [26]. Similarly, fluorescence correlation spectroscopy can be used to measure surface diffusion [27], but is susceptible to the same issues involving adsorption to and desorption from the surface. On the other hand, total internal reflectance fluorescence microscopy (TIRFM), when used to track individual molecular trajectories, can explicitly identify and distinguish surface adsorption, diffusion, and desorption processes for every individual molecule that

adsorbs to the surface. Our group has exploited single-molecule TIRFM to determine mechanisms of surfactant behavior at the solid-liquid interface, including activation energies of adsorption [28,29] and interfacial diffusion [8], consequences of surface heterogeneity [30], and multiple diffusive modes related to molecular conformation [24].

In this Letter, we present the results of single-molecule TIRFM measurements of the dynamics of a fluorescently labeled surfactant on both homogenous and heterogeneous hydrophobic surfaces. By exploiting surface features of the heterogeneous (i.e. ''patchy'') trimethylsilyl surface, we show directly that adsorbate molecules exhibit both a slow surface diffusion mode (crawling) and a desorption-mediated fast mode of diffusion (flying), and describe these modes quantitatively.

Surfaces were prepared by photodegradation of hydrophobically modified fused silica (FS) surfaces [30]. A 50 mm-diameter FS wafer (MTI Corp.) was cleaned in hot piranha solution for ~1 h followed by UV-ozone treatment for another ~60 min. The clean hydrophilic substrate was placed in a sealed glass container containing hexamethyldisilazane (HMDS, 99.8% purity, Acros Organics) and positioned ~5 cm above the liquid to expose its surface to HDMS vapor for ~48 h. In contrast with solution deposition of SAMs, this vapor-deposition process ensured that the trimethylsilyl (TMS) layer contained no fluorescent impurities as confirmed by control TIRFM experiments carried out with pure deionized water (Millipore, Milli-Q UV, 18.3 $M\Omega \cdot cm$). These TMS-modified surfaces were then exposed for the desired degradation time to UV illumination from a Hg pen lamp (UVP 254 nm) held ~5 mm from the surface. The intensity was ~0.3 mW/cm^2 at this distance. The surfaces were then exposed to solutions of fluorescently labeled dodecanoic acid (Invitrogen Bodipy® FL-C_{12}) at concentrations of 2×10^{-13} M for photodegraded TMS surfaces and 2×10^{-15} M for TMS surfaces. A time series of TIRFM images was obtained by continuous sampling for 7 min, with each frame having an exposure time of 400 ms.

Figure 1 shows the cumulative (i.e., integrated) squared-displacement distribution, $C(r^2, t)$, of the dodecanoic acid molecules on a uniform TMS surface. On this semilog plot, a straight line would indicate a single Gaussian mode of diffusion. However, the systematic deviation from the best fit to a single exponential (dashed line in Fig. 1) indicates that multiple modes of diffusion are needed to describe the trajectories. The overall surface diffusion is a weighted average of these different modes of diffusion, where the weights are the fraction of steps in each mode. A double exponential (solid line in Fig. 1) provides satisfactory agreement with the data. This analysis suggests that there is a fast mode ($D_{fast} = 0.153 \pm 0.001$ $\mu m^2/s$) that corresponds to 90% of the displacements, and a slow mode ($D_{slow} = 0.019 \pm 0.003$ $\mu m^2/s$) representing the remaining 10% of displacements.

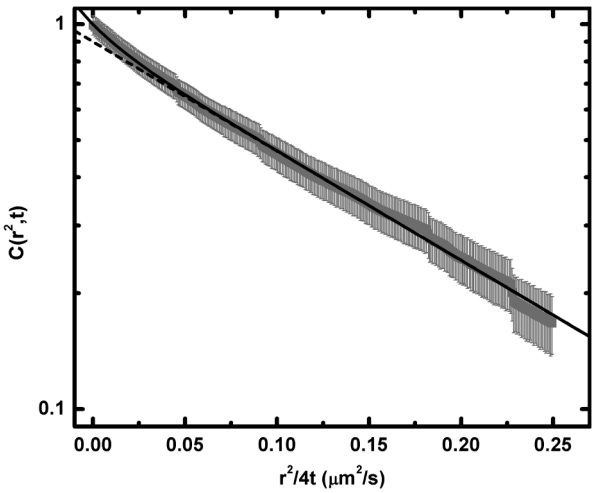

FIG. 1. Cumulative squared-displacement distribution for dodecanoic acid on a trimethylsilyl surface. The dashed and solid lines correspond to single-exponential and double-exponential fits as described in the text.

Multiple modes of diffusion are common for interfacial diffusion [8,20,24,31], and can be due to a number of factors including multiple binding modes, molecular conformations, lateral heterogeneity, etc. For the gas-liquid and liquid-liquid interfaces, theoretical models involving modifications of Stokes-Einstein diffusion for 2D systems [32,33] provide a direct connection between a diffusion coefficient and the apparent hydrodynamic radius. This connection has been exploited to determine molecular conformations associated with interfacial diffusion coefficients at the oil-water interface [21]. However, the solid-liquid interface has no such theoretical model directly linking a particular diffusive mode to a specific molecular mechanism. Such a connection requires additional information beyond the diffusion coefficient itself. For example, in previous work studying interfacial diffusion of proteins at the solid-liquid [31] and liquid-liquid [21] interfaces, the fluorescence intensity and surface residence times of protein objects were correlated with diffusion to determine that diffusion modes were primarily associated with the oligomer state of the protein. In another study with fatty acids diffusing at the solid-liquid interface [24], the temperature dependence of diffusion showed that one mode of diffusion was an Arrhenius activated process. In the current work, the heterogeneity of the surface itself was used to determine the mechanism of the fast diffusion mode.

As shown in Fig. 2, MAPT (Mapping Accumulated Probe Trajectories) was used to characterize the spatial heterogeneity of partially degraded hydrophobic surfaces. MAPT is a superresolution imaging technique [34] based on distributing the various accumulated properties of many single-molecule trajectories (adsorption, diffusion, desorption, etc.) into spatial areas and then computing spatial maps of these properties. In Fig. 2(a), a MAPT image of surface coverage shows the spatial density of accumulated

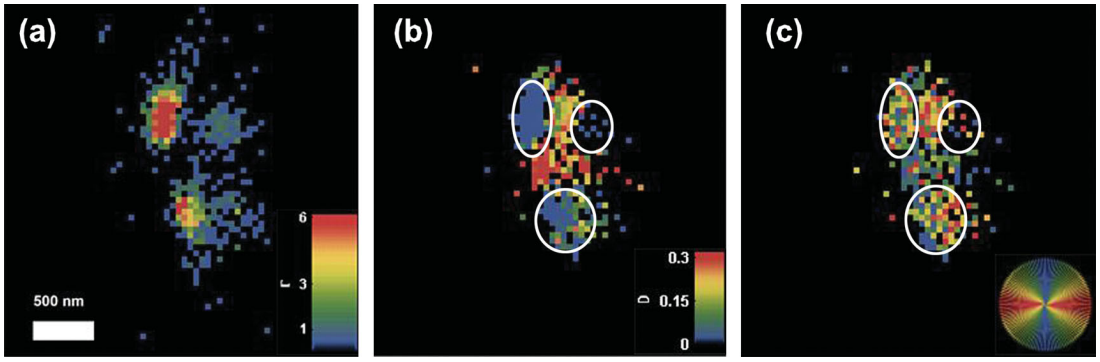

FIG. 2 (color). MAPT images of (a) surface coverage (10^{-12} $\mu m^{-2} s^{-1} M^{-1}$), (b) diffusion magnitude ($\mu m^2/s$), and (c) diffusion direction for a selected region of the degraded TMS surface.

molecular positions on a small region of the surface. In this image, we see three local regions where the molecules reside, with gaps in between where the molecules are never present on the surface. The white outlines in Figs. 2(b) and 2(c) provide guides to the eye to represent these areas of high coverage. The high-coverage regions on the degraded TMS surface represent areas of higher residual hydrophobicity, as previously predicted by simulation [35], while the regions of low coverage represent hydrophilic ''bare'' fused silica regions from which the TMS monolayer has been removed [34]. In Fig. 2(b), a MAPT image shows the magnitude of the local diffusion coefficient. It is important to note that, by convention, the diffusion coefficient is mapped at the midpoint of displacements, not at recorded molecular locations. In Fig. 2(b), six distinct regions are present, with slow diffusion (blue and green) on the regions corresponding to high surface coverage [from Fig. 2(a), marked by white outlines] and fast diffusion (yellow and orange) directly between the high-coverage regions, in areas with little or no surface coverage. In Fig. 2(c), a MAPT image of direction shows the average direction of the local diffusion coefficient, using a color coded ''compass'' showing whether the displacements are in the vertical direction (blue and green) or horizontal direction (red and yellow). In Fig. 2(c), the displacements within the high-coverage regions (marked by white outlines) have random directions. However, the displacements in-between the high-coverage regions are consistently horizontal (between the two regions on top) or vertical (between the lower region and both of the regions above). The combined evidence from the magnitude and direction of these diffusive steps associated with regions of no surface coverage indicates that they are due to displacements that started in one region of high surface coverage and ended in another region of high surface coverage. By definition, these displacements are desorption-mediated displacements (flying mode), because molecular positions are never recorded for most of the region where the flying mode of diffusion occurs.

An important experimental consideration involves the question of whether the apparent flying mode displacements are, in fact, an artifact due to coincidental desorption of one molecule and adsorption of another molecule in consecutive movie frames. We have addressed this question statistically by calculating the expected number of such ''coincidental events'' based on independent measurements of adsorption and desorption rates. In Fig. 3(a), a lower magnification MAPT image of the surface shows many areas of high surface coverage (orange in color), similar to the areas magnified in Fig. 2(a), present throughout the surface. The mean adsorption rate (0.5 ± 0.3 molecules s^{-1} μm^{-2}) and desorption rate

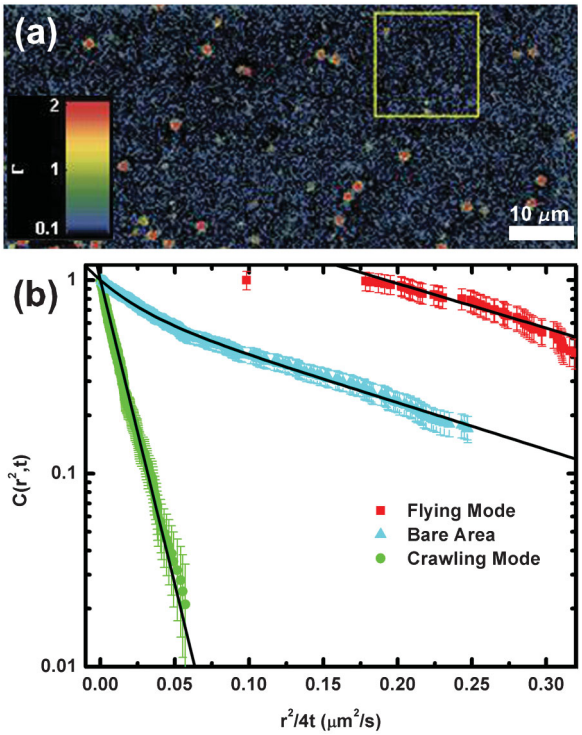

FIG. 3 (color). (a) MAPT image of surface coverage (10^{-12} $\mu m^{-2} s^{-1} M^{-1}$) with a relatively uniform area denoted by the yellow box. (b) Cumulative squared-displacement distribution for flying mode, crawling mode from Fig. 2, and bare area denoted by the yellow box in (a).

(0.65 ± 0.47 molecules s^{-1}) was measured for 28 of these regions. Using these adsorption and desorption rates for two independent adsorption sites, 100 stochastic simulations were performed to determine the number of coincidental desorption and adsorption events in consecutive frames. In our simulations, we allowed for multiple molecules to exist on one adsorption site at the same time, with independent desorption. We calculated 1.0 ± 1.0 coincidental events per experiment in the simulations, compared to the 98 observed flying displacements between the two regions on the left in Fig. 2(a). Therefore, apparent flying mode displacements due to coincidental events represent a negligible fraction of the total number of observed events.

It is interesting to compare the magnitudes of the crawling and flying modes found in Fig. 2(a) (that are characterized on a local region of extremely high surface coverage) to diffusion within uniform areas of the degraded TMS surface, representative of the majority of the surface area. Figure 3(b) shows the cumulative squared-displacement distributions for the steps between regions of high coverage (flying mode), the steps within regions of high coverage (crawling mode), and all steps within a large area of uniform surface coverage that is denoted by the yellow box in Fig. 3(a). The uniform area exhibits both slow ($D_{slow} = 0.026 \pm 0.001$ $\mu m^2/s$) and fast ($D_{fast} = 0.179 \pm 0.002$ $\mu m^2/s$) diffusive modes that are similar in magnitude to those observed on the undegraded TMS surface (Fig. 1). The degraded TMS surface, however, exhibits a larger fraction (30%) of slow-mode displacements than does the undegraded TMS surface (10%). Interestingly, D_{slow} and D_{fast} correspond closely to the apparent diffusion coefficients of the crawling and flying modes, respectively. In particular, the apparent crawling mode diffusion coefficient within high-coverage areas (0.0138 ± 0.0001 $\mu m^2/s$) was within a factor of 2 of D_{slow}, and the flying mode diffusion coefficient (0.18 ± 0.03 $\mu m^2/s$) was equal to D_{fast} within experimental uncertainty. We note that the flying mode apparent diffusion coefficient was calculated from the slope of the cumulative step size distribution in the range of 0.175 to 0.300 $\mu m^2/s$ to avoid artifacts due to the depletion of small step sizes from the geometrical constraints of the system in Fig. 2.

Table I summarizes the values of all diffusion coefficients described in this manuscript. We see that for all the surfaces and features, there are two distinct diffusion regimes that differ by an order of magnitude. The slow regime consists of the slow mode of the undegraded TMS, the slow mode of the degraded TMS uniform area, and the crawling mode diffusion within confined regions of high coverage. The fast regime consists of the fast mode of undegraded TMS, the fast mode of the degraded TMS uniform area, and the flying mode diffusion between regions of high coverage. Based on these values, we infer a mechanistic connection between the diffusive modes corresponding to these two widely separated regimes of mobility, in particular, that the modes on uniform surfaces represented by D_{slow} are in fact crawling modes and that the modes on uniform surfaces represented by D_{fast} are flying modes (desorption-mediated surface diffusion). The large fractions corresponding to the fast diffusive mode on both the uniform TMS surface (90%) and the degraded TMS surface (71%) suggest that desorption-mediated diffusion is the dominant form of surface transport for fatty acids on these surfaces.

While we have primarily looked at low concentration solutions, this flying mode should be relevant over a wide range of bulk solution concentrations. The surface concentration of surfactant (which is dependent on bulk concentration) is the most important parameter in determining the relative importance of the two modes of diffusion. At low surface concentrations, the flying mode is clearly the dominant mode of surface transport. However, at high surface concentrations the situation is less clear. For example, we hypothesize that at high surface concentrations, desorption from the surface may be significantly impeded by lateral interactions with other surfactants. The crawling mode is also likely to be slowed due to increased crowding or drag by neighboring surfactant molecules. The effects of surface crowding on the dynamics (adsorption, desorption, and diffusion will all be affected) of molecular-surface interactions cannot be inferred from the data presented in this letter and should be the focus of future experiments.

As mentioned previously, desorption-mediated surface diffusion has been theoretically described for both solid-liquid and liquid-liquid interfaces [9]. This theoretical model predicts a deviation from typical Gaussian distributions of step sizes due to the apparent Levy flights performed by the molecules when projected onto the surface plane. Specifically, the probability distribution of displacements was predicted to be a Cauchy distribution

TABLE I. Summary of diffusion results for TMS surfaces and regions of interest.

Surface/feature	Fraction of displacements	$D(\mu m^2/s)$
TMS	0.90 ± 0.01	0.153 ± 0.001
	0.10 ± 0.01	0.019 ± 0.003
Degraded TMS uniform area	0.71 ± 0.01	0.179 ± 0.002
	0.29 ± 0.01	0.026 ± 0.001
Degraded TMS crawling mode	1.0	0.0138 ± 0.0001
Degraded TMS flying mode	1.0	0.18 ± 0.03

characterized by an effective "speed" $c = D/h$, where c is the speed, D is the diffusion coefficient in the liquid phase, and h is the surface displacement length. Our experimental data are in better agreement with a Gaussian model; however, using a fit to the Cauchy distribution, we estimate the effective speed to be $c = 0.47\ \mu\text{m/s}$ in the context of this theory. It is possible that the deviation of our experimental data from the Cauchy distribution may be due to acquisition time effects, i.e., that observed flying displacements actually represent a time-weighted average of desorption-mediated and crawling displacements.

The dominance of desorption-mediated diffusion has important implications for many surface processes, but the example of self-assembled monolayer growth kinetics provides a unique opportunity to make connections between the current findings and previous experimental estimates of surface diffusion. Kinetic "population-balance" models are widely used to describe cluster nucleation and growth in epitaxial films [36–39] or self-assembled monolayers [1,2]. Using these models, the surface diffusion coefficient can be estimated from the nucleation and growth rates of small patches of self-assembled surfactants during the growth of a self-assembled surfactant monolayer. The surface diffusion coefficient for octadecylphosphonic acid on mica [2] was estimated to be $0.29 \pm 0.03\ \mu\text{m}^2/\text{s}$, which is larger but still within a factor of 2 of the flying mode of diffusion measured in our system. Given the similarity of these systems, the crawling mode (which exhibits an order of magnitude lower diffusion coefficient) would be an unlikely mechanism for a diffusion coefficient that is faster than the flying mode in our system. The similarity of the diffusion coefficients suggests that the flying mode is the main mechanism of diffusion associated with the formation of self-assembled monolayers.

This work was supported by the U.S. National Science Foundation (CHE 0841116) and the U.S. Department of Energy (DE-0001854).

*To whom communication should be addressed.
daniel.schwartz@colorado.edu

[1] I. Doudevski, W. A. Hayes, and D. K. Schwartz, Phys. Rev. Lett. **81**, 4927 (1998).
[2] I. Doudevski and D. K. Schwartz, J. Am. Chem. Soc. **123**, 6867 (2001).
[3] C. E. Allen and E. G. Seebauer, J. Chem. Phys. **104**, 2557 (1996).
[4] R. I. Cukier, J. Chem. Phys. **79**, 2430 (1983).
[5] D. Axelrod and M. D. Wang, Biophys. J. **66**, 588 (1994).
[6] V. Chan, D. J. Graves, and S. E. McKenzie, Biophys. J. **69**, 2243 (1995).
[7] A. M. Lieto, B. C. Lagerholm, and N. L. Thompson, Langmuir **19**, 1782 (2003).
[8] A. Honciuc, A. W. Harant, and D. K. Schwartz, Langmuir **24**, 6562 (2008).
[9] O. V. Bychuk and B. O'Shaughnessy, Phys. Rev. Lett. **74**, 1795 (1995).
[10] T. Adalsteinsson and H. Yu, Langmuir **16**, 9410 (2000).
[11] P. C. Ke and C. A. Naumann, Langmuir **17**, 5076 (2001).
[12] A. D. Malec *et al.*, Langmuir **20**, 1305 (2004).
[13] C. Selle *et al.*, Phys. Chem. Chem. Phys. **6**, 5535 (2004).
[14] K. Tamada, S. H. Kim, and H. Yu, Langmuir **9**, 1545 (1993).
[15] K. Tanaka *et al.*, Langmuir **15**, 600 (1999).
[16] K. Tanaka and H. Yu, Langmuir **18**, 797 (2002).
[17] F. Hashimoto, S. Tsukahara, and H. Watarai, Langmuir **19**, 4197 (2003).
[18] M. Negishi *et al.*, Langmuir **24**, 8431 (2008).
[19] G. J. Schütz, H. Schindler, and T. Schmidt, Biophys. J. **73**, 1073 (1997).
[20] R. Walder, A. Honciuc, and D. Schwartz, J. Phys. Chem. B **114**, 11 484 (2010).
[21] R. Walder and D. K. Schwartz, Langmuir **26**, 13 364 (2010).
[22] R. Walder and D. K. Schwartz, Soft Matter **7**, 7616 (2011).
[23] K. D. Dobbs and D. J. Doren, J. Chem. Phys. **97**, 3722 (1992).
[24] A. Honciuc and D. K. Schwartz, J. Am. Chem. Soc. **131**, 5973 (2009).
[25] C. E. Heitzman, H. L. Tu, and P. V. Braun, J. Phys. Chem. B **108**, 13 764 (2004).
[26] C. F. Schmidt, R. M. Zimmermann, and H. E. Gaub, Biophys. J. **57**, 577 (1990).
[27] P. Burgos *et al.*, ACS Nano **3**, 3235 (2009).
[28] A. Honciuc *et al.*, Langmuir **25**, 7389 (2009).
[29] A. Honciuc, A. L. Howard, and D. K. Schwartz, J. Phys. Chem. C **113**, 2078 (2009).
[30] A. Honciuc, D. J. Baptiste, and D. K. Schwartz, Langmuir **25**, 4339 (2009).
[31] M. Kastantin *et al.*, J. Am. Chem. Soc. **133**, 4975 (2011).
[32] B. D. Hughes, B. A. Pailthorpe, and L. R. White, J. Fluid Mech. **110**, 349 (1981).
[33] P. G. Saffman and M. Delbruck, Proc. Natl. Acad. Sci. U.S.A. **72**, 3111 (1975).
[34] R. Walder, N. Nelson, and D. K. Schwartz, Nature Commun. (to be published).
[35] H. Acharya *et al.*, Faraday Discuss. **146**, 353 (2010).
[36] J. G. Amar and F. Family, Phys. Rev. Lett. **74**, 2066 (1995).
[37] J. G. Amar and F. Family, Thin Solid Films **272**, 208 (1996).
[38] J. A. Venables, Philos. Mag. **27**, 697 (1973).
[39] J. A. Venables *et al.*, Rep. Prog. Phys. **47**, 399 (1984).